

## Gum Metal under cyclic tension inspected by a fast and sensitive infrared camera

by K.M. Golasiński\*, E. Pieczyska\*, M. Maj\*, M. Staszczak\* and S. Kuramoto\*\*

\* Institute of Fundamental Technological Research, Polish Academy of Sciences, Pawińskiego 5B, 02-106, Warsaw, Poland, e-mail: [kgolasin@ippt.pan.pl](mailto:kgolasin@ippt.pan.pl)

\*\* Department of Mechanical Engineering, College of Engineering, Ibaraki University, 316-8511, Hitachi, Japan, e-mail: [shigeru.kuramoto.11@vc.ibaraki.ac.jp](mailto:shigeru.kuramoto.11@vc.ibaraki.ac.jp)

### Abstract

This work presents results of experimental investigation of recoverable deformation of a  $\beta$ -Ti alloy Gum Metal inspected by infrared (IR) thermography. To this end, a flat specimen of Gum Metal was subjected to cyclic tension with an increasing strain on a testing machine and was simultaneously monitored by a fast and sensitive IR camera. The IR measurements determined an average temperature accompanying the alloy deformation process for subsequent tension cycles and allowed to estimate thermoelastic effect, which is related to the alloy yield point. Thermomechanical couplings accompanying the loading-unloading cycles were analyzed for estimating the range of reversible deformation from mechanical and thermal perspectives as well as discussed in the view of Lord Kelvin's formula.

### 1. Introduction

Gum Metal is a multifunctional set of  $\beta$ -Ti alloys with outstanding properties developed at the Toyota Central R&D Labs., Inc.. Gum Metal with a typical composition Ti-23Nb-0.7Ta-2Zr-1.2O (at.%) is fabricated by subsequent processes of powder sintering, solution treatment and cold working. The technological procedure and the chemical composition of Gum Metal result in a combination of low elastic modulus, superelastic-like performance, high strength, superplastic behavior as well as Elinvar- and Invar- like thermal stability [1]. The unusual properties and high elastic-plastic behavior of the alloy has attracted significant interest of scientists and engineers in the past decade. In particular, the large non-linear recoverable deformation of Gum Metal has been a focal point of several investigations. The unconventional deformation mechanisms responsible for this peculiar behavior have been intensively studied [2-10]. Recent articles suggest that activity of phase transformations is of key importance for the nonlinear superelastic-like deformation of Gum Metal. However, the long-range martensitic transformation was explained to be suppressed by a specific oxygen content. Advanced microstructural analyses found a presence of nanodomains of martensite and precipitations of omega phase in Gum Metal [4, 5]. Both of the phases are of order of few nanometers [6,7]. Most probably, the stress-induced growth of martensitic nanodomains is the underlying deformation mechanism of the nonlinear recoverable strain of Gum Metal [7-10]. However, some reports [4,6] suggest that omega precipitates can play a role in this deformation stage as well.

In this study, measurements of exothermic character of the stress-induced activity of martensite nanodomains and/or omega phase using IR technique allowed to contribute to the research on unique properties of Gum Metal. A major focus of this research was to investigate the recoverable deformation of Gum Metal from mechanical and thermodynamic perspectives.

### 2. Experimental details

A photo and a scheme of the experimental set-up used in this study are shown in Figs.1a and 1b, respectively. Shape and dimensions of the Gum Metal specimen are presented in Fig. 1c. The specimen of Gum Metal was provided by Toyota Central R&D Labs., Inc.. The composition of Gum Metal was Ti-23Nb-0.7Ta-2Zr-1.2O (at.%) and the fabrication included the steps described in [1].

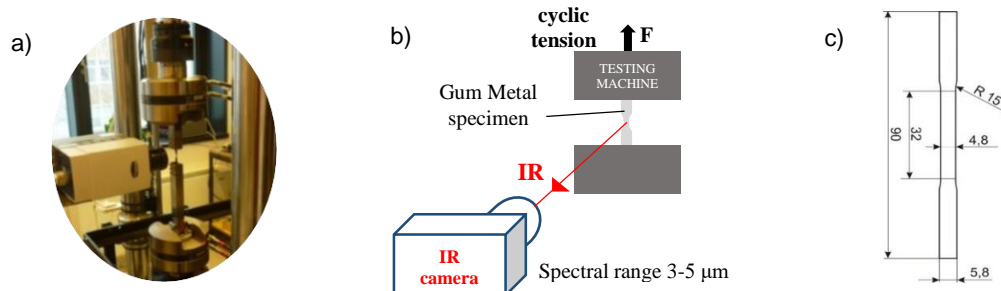


Fig. 1: Experimental set-up: a) photo; b) scheme; c) shape and dimensions of Gum Metal specimen.

In the present study, on the one hand, cyclic tension on a testing machine MTS 858 was performed at the strain rate of  $4 \times 10^{-4} \text{ s}^{-1}$  in order to determine the mechanically reversible deformation range of the alloy. The strain measurements were conducted using a mechanical extensometer. The loading-unloading subsequent cycles were performed with a strain step of  $\Delta \varepsilon = 0.002$ . On the other hand, the fast and sensitive IR camera Flir Co Phoenix was monitoring the Gum Metal specimen subjected to subsequent loading-unloading cycles and served to obtain the thermal response of the alloy based on the distribution of IR radiation emitted by the specimen's surface. Before the loading, the specimen of Gum Metal was covered with soot for determination of absolute temperature. The emissivity coefficient of the soot equal to 0.95 was assumed. The camera parameters used in the experiment were as follows: a wave length range  $3 \mu\text{m} \div 5 \mu\text{m}$ , maximal recording frequency 538 Hz, window size  $160 \times 256$  pixels, thermal sensitivity up to  $0.02 \text{ }^\circ\text{C}$ . The IR parameters are listed in Table 1.

**Table 1.** Parameters of the IR camera Flir Co Phoenix.

IR Camera	wave length range	maximal recording frequency	window size	thermal sensitivity
Flir Co Phoenix	$3 \mu\text{m} \div 5 \mu\text{m}$	538 Hz	$160 \times 256$ pixels	up to $0.02 \text{ }^\circ\text{C}$

The average temperature change  $\Delta T$  was determined with high thermal sensitivity up to  $0.02 \text{ K}$  based on the captured IR distributions. The average temperature change  $\Delta T$  denotes the difference between the average value of the temperature calculated for the gauge area of the specimen at each instant of loading  $T(t)$  and the average temperature of the same area before the deformation  $T(t_0)$ , as expressed by Eq. (1).

$$\Delta T = T(t) - T(t_0). \quad (1)$$

### 3. Results and discussion

#### 3.1. Analysis of true stress vs. true strain curves for Gum Metal under cyclic tension

True stress vs. true strain curves plotted for Gum Metal subjected to cyclic tension at the strain rate of  $4 \times 10^{-4} \text{ s}^{-1}$  on the testing machine are presented in Fig. 2. The first cycle was realized within a strain of 0.002 and subsequent cycles were performed with a strain step of  $\Delta \varepsilon = 0.002$ . The experiment consisted of 14 tension loading-unloading cycles. The rupture of the Gum Metal specimen occurred in cycle 14. High elastic characteristics of Gum Metal namely low Young's modulus (around 62 GPa) as well as the nonlinear superelastic-like deformation and recoverable strain of around 0.014 were confirmed. High strength of Gum Metal (over 1000 MPa) was observed for cycles 10-14, in which the specimen was apparently deformed in plastic regime.

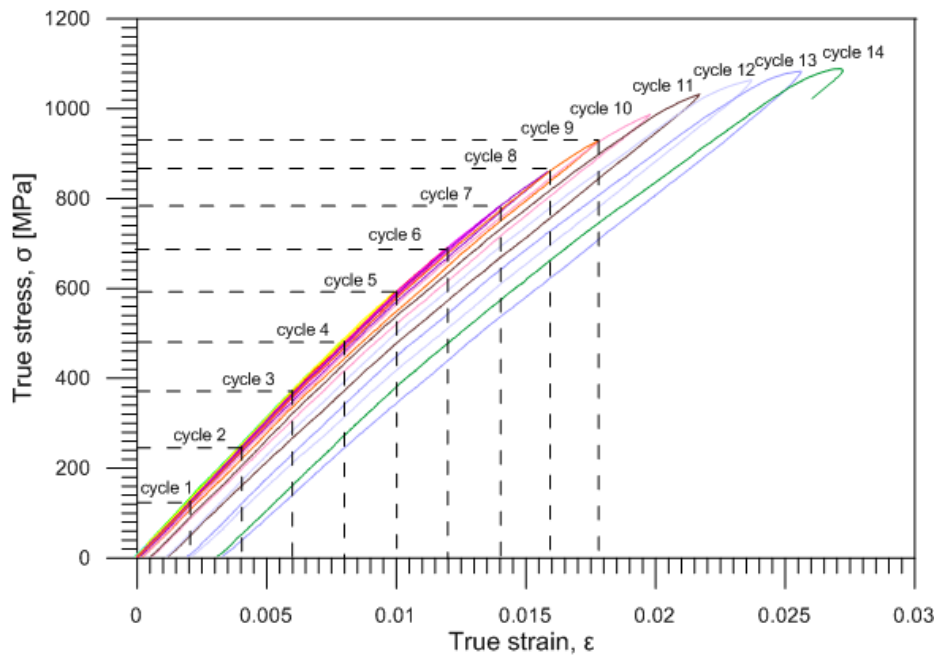


**Fig. 2:** True stress vs. true strain curves for Gum Metal under cyclic tension at strain rate of  $4 \times 10^{-4} \text{ s}^{-1}$  with a strain step  $\Delta \varepsilon = 0.002$ .

### 3.2. Analysis of true stress and temperature change vs. true strain curves for Gum Metal under cyclic tension

True stress and the related temperature change vs. true strain curves obtained for initial loading-unloading tensile cycles 1, 2 and 3 of Gum Metal are shown in Figs. 3 a, b, c. On the one hand, the true stress vs. true strain plots in the loading-unloading process overlap for cycles 1 – 3. It means that the strain is totally recoverable from the mechanical perspective for these cycles. On the other hand, the temperature change vs. true strain decreases during the loading stage in cycles 1 - 3.

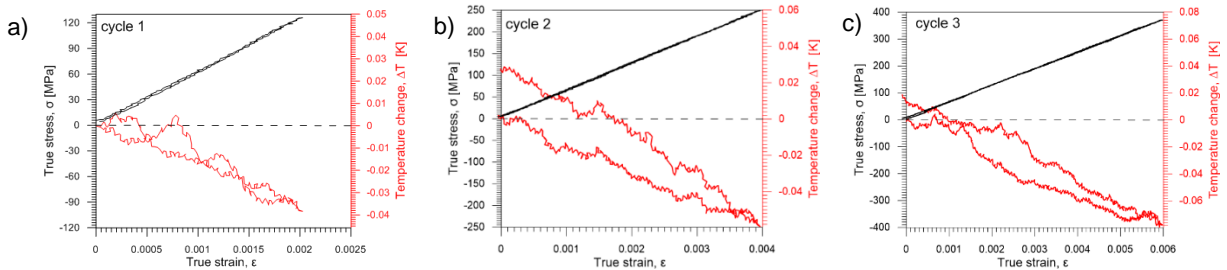


**Fig. 3:** True stress and temperature change vs. true strain curves for tensile cycles of Gum Metal: a) cycle 1, b) cycle 2 and c) cycle 3.

The thermal responses of Gum Metal observed during loading for cycles 1 - 3 are in line with Lord Kelvin's formula expressed by Eq. (2).

$$\Delta T = -\alpha \frac{T \Delta \sigma_s}{c_\sigma}, \quad (2)$$

where:

$\alpha$  – the coefficient of linear thermal expansion,

$T$  – the initial absolute temperature,

$c_\sigma$  – the heat capacity per unit volume at constant stress,

$\Delta \sigma_s$  – the change of stress (change in the uniaxial stress tensor).

In general, deformation of any material is accompanied by its temperature change. This phenomenon is called thermoelastic effect [11]. During elastic deformation of the material with a positive coefficient of thermal expansion subjected to tension under adiabatic conditions, its temperature decreases. Temperature variation of the material under loading is a result of conversion of the potential and kinetic energy of lattice atoms. Thus, an analysis of thermal response of a material under loading can serve to determine a range of elastic deformation [11-13]. During plastic deformation the temperature of tested material grows due to dissipative processes related to change in the structure.

In subsequent cycles 4, 5 and 6, the true stress vs. true strain plots in the loading-unloading process still overlap so the strain is recoverable, as shown in Fig. 4 a - c. However, the temperature change vs. true strain during loading firstly decreases and then slightly increases in the final phase of Gum Metal loading. The minimum value of temperature variation, which is equal to -0.08K, can indicate the range of purely elastic deformation of Gum Metal. It corresponds to the strain value of 0.007.

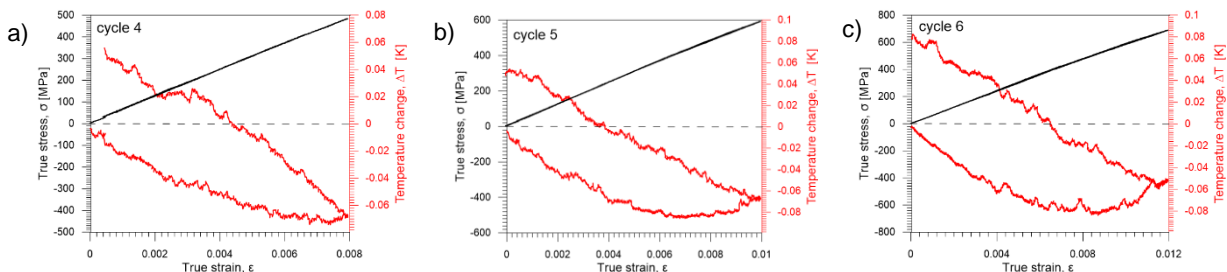


**Fig. 4:** True stress and temperature change vs. true strain curves for subsequent tensile cycles of Gum Metal: a) cycle 4, b) cycle 5 and b) cycle 6.

True stress and temperature change vs. true strain curves obtained for tensile cycles 7 - 9 of Gum Metal are shown in Figs. 5 a - c. Maximal recoverable strain of Gum Metal was observed in cycle 7 for strain of 0.014. In cycles 8 and 9, on one hand true stress vs. true strain curves do not overlap and an hysteresis is noticed. On the other hand, there is a significant temperature growth in the final stage of loading which accompanies the plastic deformation of Gum Metal.

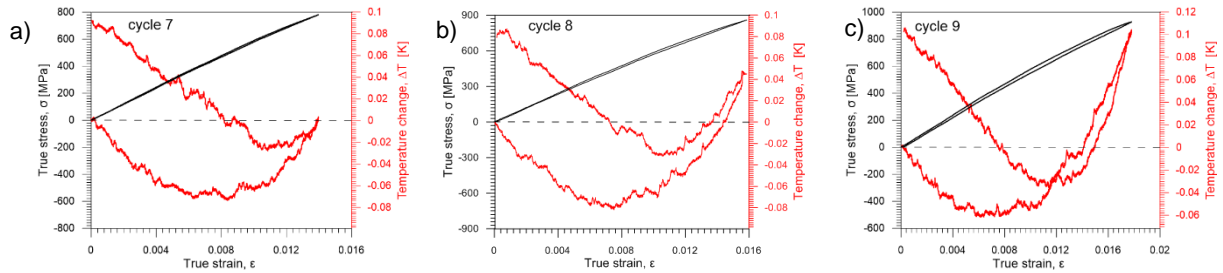


**Fig. 5:** True stress and temperature change vs. true strain curves for tensile cycles of Gum Metal: a) cycle 7, b) cycle 8 and b) cycle 9.

Firstly, it was estimated that the mechanically reversible deformation was present until performing cycle 7 within the strain range 0.014, as seen in Fig. 5a. Secondly, the maximal temperature drop  $\approx -0.08\text{K}$  in the Gum Metal specimen under cyclic tension corresponds to the strain of around 0.007 (Fig. 4a). Thus, the thermodynamic nature of the mechanically estimated recoverable strain indicates a combination of two stages: elastic deformation and a nonlinear stage accompanied by a temperature growth. The latter demonstrates an exothermic nature of such a large reversible strain range of Gum Metal. This phenomenon is believed to originate from other deformation mechanisms such as stress-induced exothermic phase transformations of martensite nanodomains and/or omega phase, which cause an apparent dissipative behavior. These unconventional deformation mechanisms were a subject of debate in several studies [4-10, 14, 15].

True stress and temperature change vs. true strain curves for tensile cycles 10 - 14 of Gum Metal are shown in Figs. 6 a - e. In cycles 10 - 13, the presented plots reveal an evident plastic deformation which is accompanied by a significant temperature change increase in the final stage of loading. Rupture of Gum Metal specimen occurred in cycle 14, at strain of around 0.27 and was accompanied by the recorded temperature change of 0.6 K.

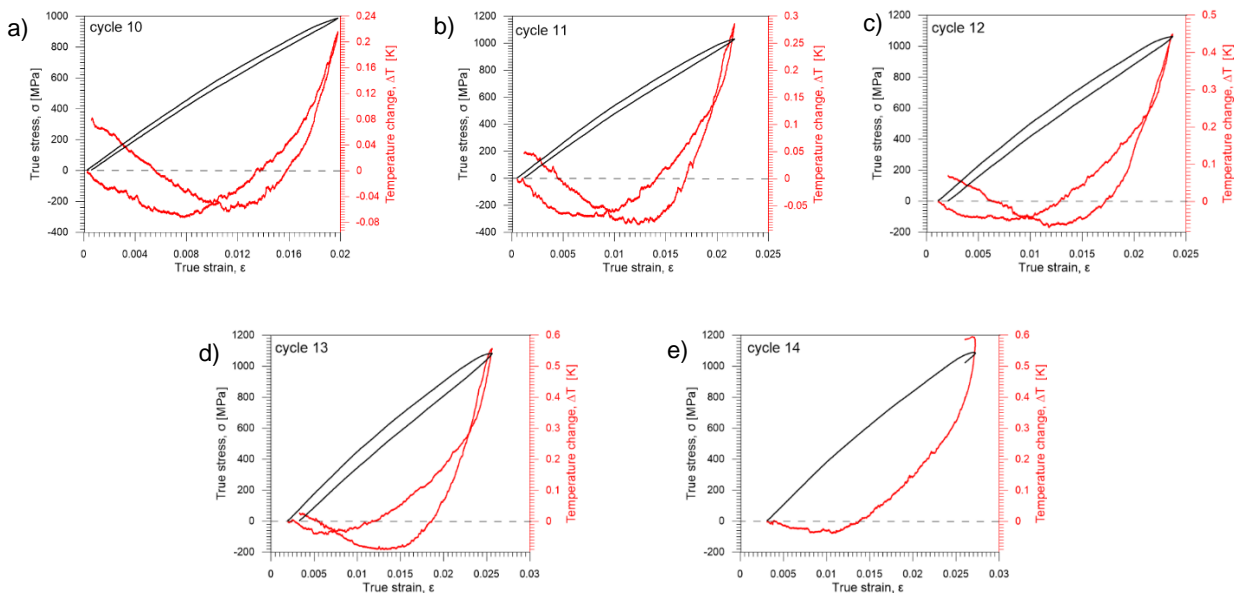


**Fig. 6:** True stress and temperature change vs. true strain curves for tensile cycles of Gum Metal: a) cycle 10, b) cycle 11, c) cycle 12, d) cycle 13 and e) cycle 14.

### 3.3. Analysis of thermograms in critical points for cycle 13 of Gum Metal cyclic tension

True stress and temperature change vs. true strain curves of Gum Metal for a representative tensile cycle 13 of advanced deformation with selected points in the temperature change curve (0) – (6) and corresponding thermograms (0)\* - (6)\* are presented in Fig. 7. The points were chosen for critical instants of the Gum Metal deformation:

- (0) beginning of loading;
- (1) minimal temperature change during loading;
- (2) maximal recoverable strain;
- (3) intermediate point of loading;
- (4) maximal temperature change;
- (5) minimal temperature change during unloading;
- (6) end of unloading.

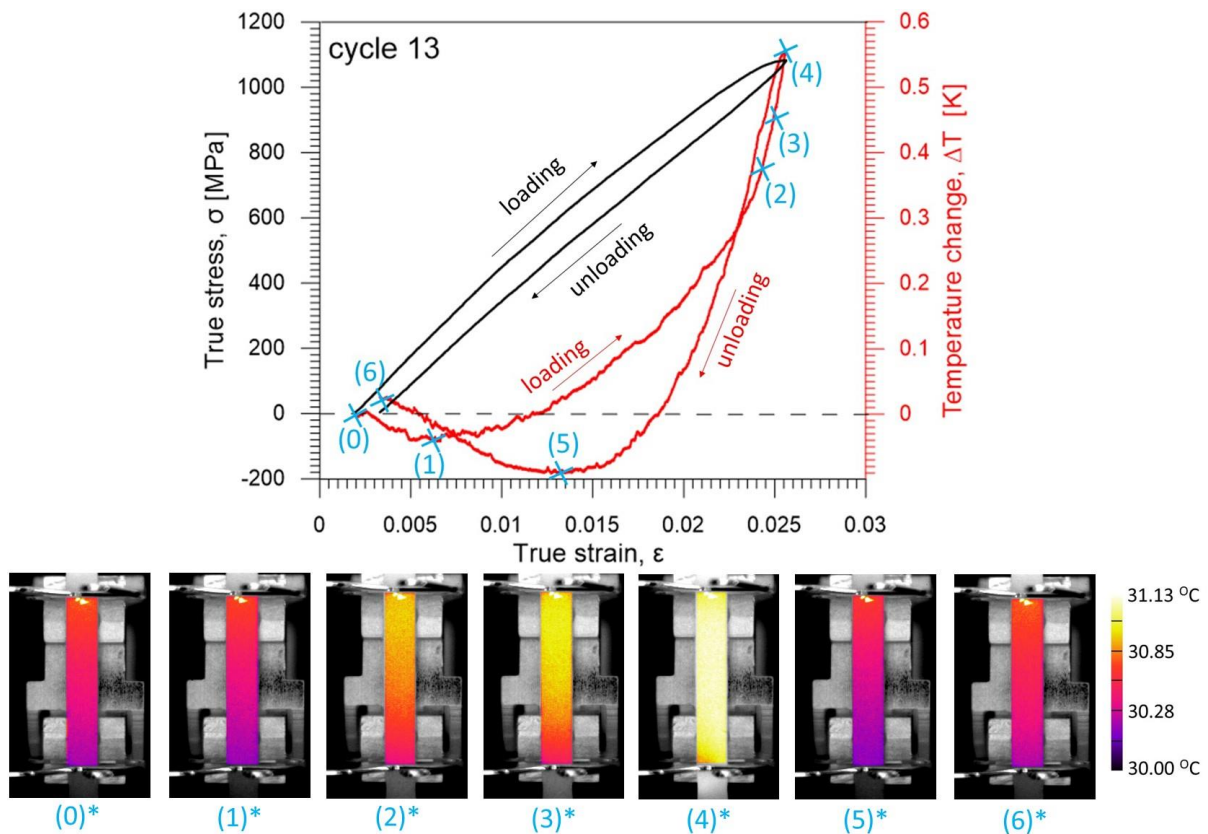


**Fig. 7.** True stress and temperature change vs. true strain curves of Gum Metal for an advanced tensile cycle 13 with selected points in the temperature change curve (0) – (6) and corresponding thermograms (0)\* - (6)\*.

In the initial phase of Gum Metal loading, a drop in temperature change is observed as shown between thermograms (0)\* and (1)\*. Purely elastic deformation of Gum Metal is observed between points (0) and (1). Further loading is accompanied by a temperature change growth caused by an activity of stress-induced martensite nanodomains and/or omega phase transformations up to point (2), as shown in (2)\*. Points (3) and (4) correspond to plastic deformation of Gum Metal with significant increase in temperature change depicted in thermograms (3)\* and (4)\*. Unloading of Gum Metal results in a drop of temperature change with minimal value in point (5), as presented in thermogram (5)\*. Cycle 13 ends in point (6) with a corresponding thermogram (6)\*. Such temperature behavior during the unloading is also related to many factors that can influence on the process, i.e. the heat exchange with the surroundings, the endothermic phase transformation, as well as its saturation (vanishing) at the final stage of the specimen unloading.

### 4. Concluding remarks

In this work, results of experimental investigation of cyclic tension of a  $\beta$ -Ti alloy Gum Metal inspected by IR thermography were presented. The thermal responses of Gum Metal were analyzed for 14 tensile cycles, which were

realized with an increasing strain. Based on Lord Kelvin's formula, a purely elastic deformation range of Gum Metal was determined. Further loading within a recoverable superelastic-like deformation revealed an exothermic nature of unconventional deformation mechanisms activated in the alloy. Plastic stage of Gum Metal loading was seen to be accompanied with a significant temperature change increase ending with rupture in cycle 14.

**Acknowledgments** The research was supported by the Polish National Science Centre under grants 2014/13/B/ST8/04280 and 2016/23/N/ST8/03688.

## REFERENCES

- [1] Saito T, Furuta T, Hwang JH, Kuramoto S, et al. Multifunctional Alloys obtained via a dislocation free plastic deformation mechanism. *Science*. 2003;300:464-467.
- [2] Kuramoto S, Furuta T, Hwang J, et al. Elastic properties of Gum Metal, *Mater. Sci. Eng. A*. 2006;442:454–457.
- [3] Golasiński KM, Pieczyska EA, Staszczak M, et al. Infrared thermography applied for experimental investigation of thermomechanical couplings in Gum Metal. *Qirt J*. 2017;14:226-233.
- [4] Yano T, Murakami Y, Shindo D, et al. Study of the nanostructure of Gum Metal using energy-filtered transmission electron microscopy. *Acta Mater*. 2009;57:628–633.
- [5] Morris Jr. JW, Hanlumyuang Y, Sherburne M, et al. Anomalous transformation-induced deformation in <110> textured Gum Metal. *Acta Mater*. 2010;58:3271–3280.
- [6] Tane M, Nakano T, Kuramoto S, Niinomi M, Takesue N, Nakajima H. Transformation in cold-worked Ti–Nb–Ta–Zr–O alloys with low body-centered cubic phase stability and its correlation with their elastic properties. *Acta Mater*. 2013;61:139–150.
- [7] Talling RJ, Dashwood RJ, Jackson M, Dye D. On the mechanism of superelasticity in Gum Metal. *Acta Mater*. 2009;57:1188–1198.
- [8] Kim HY, Miyazaki S. Several Issues in the Development of Ti–Nb-Based Shape Memory Alloys. *Shap. Mem. Superelasticity* 2016;2:380–390.
- [9] Wei LS, Kim HY, Miyazaki S. Effects of oxygen concentration and phase stability on nano-domain structure and thermal expansion behavior of Ti–Nb–Zr–Ta–O alloys. *Acta Mater*. 2015;100:313–322.
- [10] Guo W, Quadir MZ, Moricca S, Eddows T, Ferry M. Microstructural evolution and final properties of a cold-swaged multifunctional Ti–Nb–Ta–Zr–O alloy produced by a powder metallurgy route. *Mater. Sci. Eng. A* 2013;575:206–216.
- [11] Thomson W. On the thermoelastic and thermomagnetic properties of matter. *Trans. R. Soc. Edin.* 1853;20:57–77.
- [12] Chrysochoos A. Infrared thermography applied to the analysis of material behaviour: a brief overview. *Qirt J*. 2012;9(2):193–208.
- [13] Pieczyska EA. Thermoelastic effect in austenitic steel referred to its hardening. *J Theor App Mech*. 1999;2(37):281–306. Ph.D thesis.
- [14] Pieczyska EA, Maj M, Golasiński KM, Staszczak M, Furuta T, Kuramoto S. Thermomechanical Studies of Yielding and Strain Localization Phenomena of Gum Metal under Tension. *Materials*. 2018;11:1-13.
- [15] Pieczyska EA, Maj M, Furuta T, et al. Gum Metal – unique properties and results of initial investigation of a new titanium alloy – extended paper. In: Kleiber M, Burczyński T, Wilde K, Gorski J, Winkelmann K, Smakosz Ł, editors. *Advances in mechanics: theoretical, computational and interdisciplinary issues*. London: Taylor & Francis Group; 2016. p. 469–472. ISBN 978-1-138-02906-4.